Contents lists available at ScienceDirect

Materials Science & Engineering A

journal homepage: www.elsevier.com

Microstructural characterization and mechanical properties of TiB_2 reinforced Al6061 matrix composites produced using stir casting process

Y. Pazhouhanfar, B. Eghbali*

Department of Materials Science and Engineering, Sahand University of Technology, Tabriz, Iran

ARTICLE INFO

Keywords:
Al6061-TiB_2 composite
Stir casting
Microstructure
Mechanical properties

ABSTRACT

Particulate reinforced aluminum matrix composites are the most promising alternative for applications where the combination of high strength and ductility is essential. In the present study, Al-TiB_2 composites with different amounts of reinforcement (3, 6 and 9 wt%) were fabricated using stir casting method. after optimizing the process parameters such as preheating temperature, stirring speed and duration. Microstructure, mechanical properties and the fracture surfaces of tensile specimens were studied. Optical microstructure of prepared composites showed a uniform distribution of reinforcements in matrix and also SEM analysis demonstrated the strong bonding between matrix and reinforcements which is the consequence of improved wettability due to K_2TiF_6 addition and preheating of TiB_2 powder before adding to the melt. In addition to microstructure uniformity, the tensile strength of composites was improved with increasing the volume fraction of TiB_2 reinforcement particles without any significant decrease in elongation. SEM micrographs from fractured surfaces of tensile specimens approved that the ductile fracture is occurred in Al6061 alloy in all of prepared composites through nucleation and coalescence of micro-voids.

1. Introduction

Metal matrix composites (MMCs) have been considered as the most suitable candidate for application in aerospace and automobile industry due to their outstanding physical and mechanical properties such as high elastic modulus, strength and thermal stability [1–3]. MMCs provide a combination of mechanical properties of metal matrix, including high toughness and ductility, and reinforcement particles such as high stiffness and hardness [4]. In the case of particulate metal matrix composites (PMMCs) the improved mechanical properties are isotropic. Also, some improvement in thermal stability and wear resistance may be achieved by adding ceramic particle into metallic matrix [5,6]. MMCs can be produced by different techniques including powder metallurgy [7,8], stir casting [9], severe plastic deformation [10], friction stir processing and other techniques. Among the available manufacturing processes, stir casting is attractive for its economic advantages in fabricating large scale parts and its flexibility in selecting raw materials and processing conditions [11]. Meanwhile, aluminum alloys are the most widely used metallic materials as a matrix in MMCs both in research and industrial applications due to the high level of strength to weight ratio. Also, aluminum alloys are cheap compared with other lightweight materials such as magnesium and titanium. The excellent mechanical properties of aluminum alloys (strength, ductility) in conjunction with high corrosion resistance is well understood and can be modified to satisfy different requirements [12]. Among all aluminum alloys, age hardening grades (2xxx, 6xxx and 7xxx) are most common as a matrix material because the use of age hardening alloys enables further improvement in mechanical properties by different aging treatments [13]. Reinforcing the aluminum alloys with ceramic particles can contribute to activate strengthening mechanisms due to morphological changes such as grain refinement, geometrically increased density of dislocations caused by thermal incompatibilities of the matrix and reinforcements and load transfer from Al onto reinforcements [14,15]. Ceramic particles including TiC [16], B_4C [17], TiB_2 [18], Al_2O_3 [19] and SiC [20] are the most commonly used reinforcements in Aluminum matrix composites (AMCs). But, titanium diboride (TiB_2) exhibit a great advantages compared with other ceramic particles. For example SiC reacts with aluminum and forms a reaction layer at the particle-matrix interface. This reaction layer is demonstrated to be a brittle Al_4C_3 intermetallic that impairs the mechanical properties of the Al matrix composites especially at high temperatures [21]. In the same way, the magnesium existing in the form of solid solution in aluminum matrix, reacts with Al_2O_3 to form Al_2MgO_4 [22]. But TiB_2 is thermodynamically stable in molten aluminum and this allows both solid state and liquid state techniques to be used for fabrication of Al-TiB_2 composites. The combination of TiB_2 excellent properties has led to widespread use of Al-TiB_2 composites in high-tech structural and functional applications including aerospace, defense and automotive industries. However, the most common use of these materials is in the field of cut-

* Corresponding author.
Email address: eghbali@sut.ac.ir (B. Eghbali)

https://doi.org/10.1016/j.msea.2017.10.087
Received 16 August 2017; Received in revised form 24 October 2017; Accepted 25 October 2017
Available online xxx
0921-5093/

ting tools, impact-resistant facilities, crucibles, and wear-resistant coating [23]. Mechanical properties of AMCs is dependent on the intrinsic properties of matrix and reinforcement, the size, volume fraction and distribution of the reinforcement in the matrix, as well as the mutual interactions at the reinforcement–matrix interfaces. Moreover, the conventional processing methods such as casting often result in agglomeration of reinforcement particles in the matrix and as a result great reduction in mechanical properties of the produced composites. The major is reason of inhomogeneous distribution of reinforcement is poor wetting between the ceramic particles and matrix [24]. This problem can be solved through various methods such as use of surface active agents which decreases surface tension and interfacial forces [25]. For example, in Al/B_4C composites, better incorporation of ceramic particles into melt can be possible by coating of B_4C particles with Ti powder which leads to the formation of complex surface layers of TiB and TiC and development of strong interfacial bonding between B_4C and aluminum [26]. In this work Al6061-TiB_2 composites with different amounts of reinforcement (3%, 6%, and 9 wt%) were synthesized using stir casting method and the resultant microstructure and mechanical properties were investigated.

2. Materials and experimental procedures

In the present study, Al6061 alloy was used as matrix material with chemical composition shown in Table 1, and TiB_2 ceramic particles were used as reinforcement. Fig. 1 shows the SEM micrograph and EDS (Energy Dispersive Spectroscopy) analysis of TiB_2 particles. As it is seen, the size of TiB_2 particles is in the range of 2–10 μm. In this work, K_2TiF_6 was used for increasing the wettability of TiB_2 particles in Al6061 melt. The SEM micrograph and X-ray diffraction pattern of the K_2TiF_6 is also shown in Fig. 2. The addition of reinforcement particles in the Al matrix was done using stir casting machine specially designed and fabricated for this purpose. Fig. 3(a) shows the stir casting machine. This casting apparatus consisted of different parts including powder injection system, agitator made of titanium, resistant furnace, thermocouples for temperature control, alumina crucible which operates under argon atmosphere. Therefore, particulate reinforced AMCs with different percentages of TiB_2 were produced by adding a mixture of TiB_2 (3, 6, 9 wt%) and K_2TiF_6 (0.9, 1.8, 2.7 wt%). In this process, TiB_2 ceramic particles were first preheated at 250 °C for 2 h in an electric furnace. Afterwards, the temperature of resistance furnace was increased above the melting temperature of Al near 700 °C

Table 1
Chemical composition of as-cast Al6061 alloy.

Elementary	Al	Mg	Si	Fe	Cu	Cr	Ti	Mn	Zn
wt%	97.55	1.04	0.55	0.31	0.26	0.21	0.03	0.02	0.01

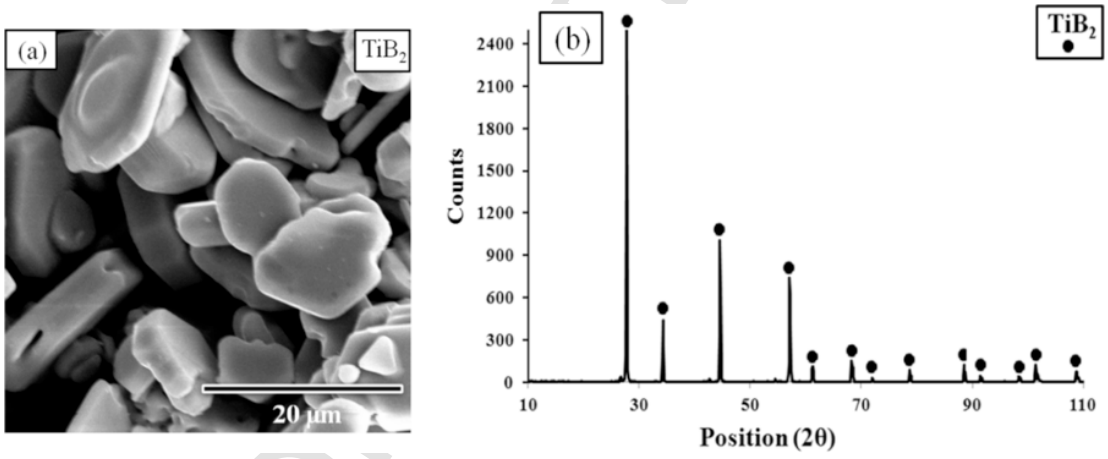

Fig. 1. (a) SEM micrograph and (b) X-Ray diffraction pattern of TiB_2 ceramic particles.

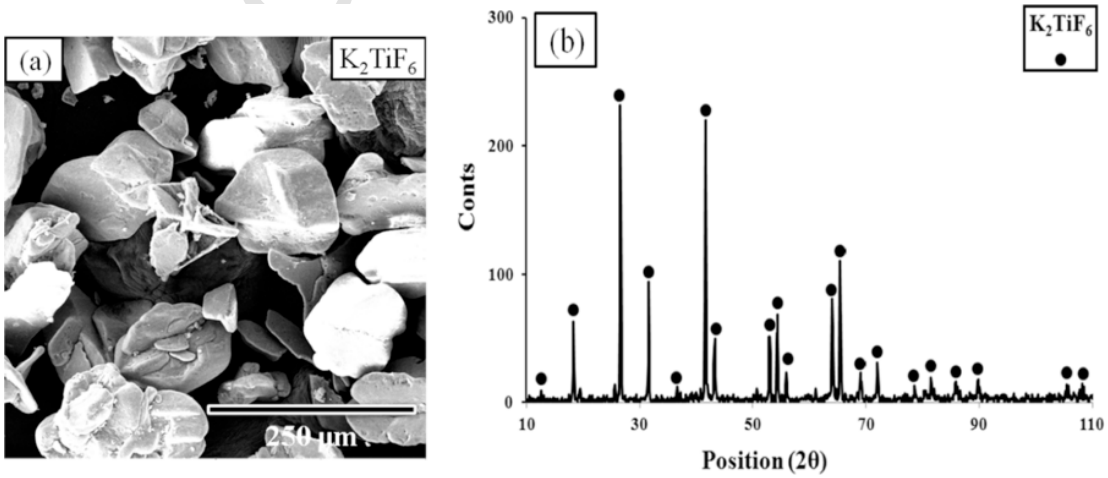

Fig. 2. (a) SEM micrograph and (b) X-Ray diffraction pattern of K_2TiF_6 particles. SEM.

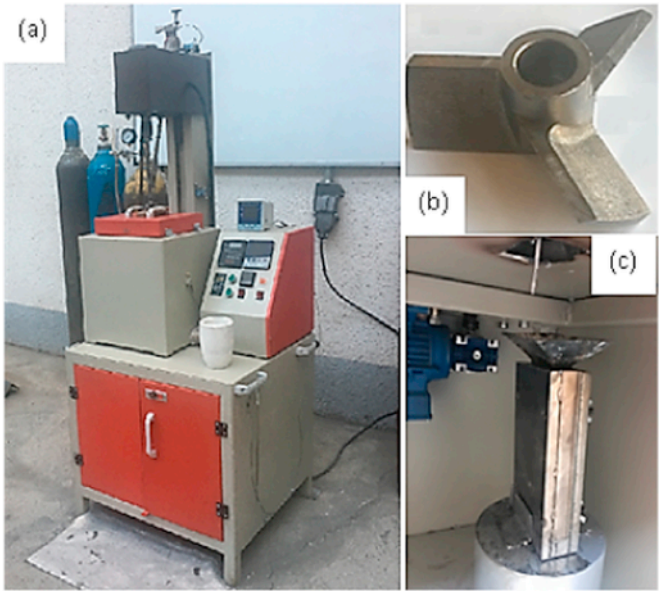

Fig. 3. (a) Stir casting machine, (b) agitator and (c) steel mold used in the present study.

to melt Al6061 completely. Preheated TiB_2 particles were then added to the melt slowly. Thereinafter, stirring was carried out in a ceramic crucible which was located inside the resistance furnace using titanium made agitator shown in Fig. 3(b). So that, the homogenous mixtures of Al6061 melt and ceramic particles were obtained after 15 min stirring with speed of 350 rpm. Also, the temperature was controlled to an accuracy of ± 5 °C using digital temperature controller. Prepared melts were instantaneously poured into the steel mold (Fig. 3(c)) which was kept at room temperature. Therefore, three cast samples with different amounts of TiB_2 were produced using the same procedure. These samples were nominated as 0, T3, T6 and T9 for 0, 3, 6 and 9 wt% of TiB_2 particles, respectively. Cast ingots were then sectioned and metallographic samples were prepared for microstructural characterization. For this purpose, the pieces of samples were mounted so that the microstructure on a selected surface can be studied. The surface of specimens was mechanically polished and etched with Keller's reagent. Optical micrographs were taken using Olympus PMG3 microscope and SEM characterization was conducted using Tescan MIRA3 field emission gun scanning electron microscope (FE-SEM) equipped with EDS. Meanwhile, X-ray diffraction patterns of Al6061 matrix and fabricated composites were acquired using Bruker D8 Advanced diffractometer for phase identification. Mechanical properties of the fabricated composites were evaluated by tensile testing at room temperature and strain rate of $4.7 \times 10^{-4}\ s^{-1}$ using GOTECH Al-7000-LA 10 tensile tester. All of the tensile tests have been performed in the same strain rate and total of three specimens were tested for each material. In addition, bending strength of composites was evaluated by three point bending tests. Also, the Vickers micro-hardness was measured by applying 25 g load for 10 s. Six micro-hardness measurements were conducted on each sample and the average values were reported for increasing reliability of results.

3. Results and discussions

3.1. Microstructure characterization

Fig. 4 shows optical micrographs of Al6061 and Al-TiB_2 composites with different amounts of reinforcements (3%, 6% and 9% TiB_2). Fig. 4(a) represents the as-casted microstructure of Al6061 alloy used as the matrix material. As can be seen, the microstructure consists of α phase and Al-Mg-Si ternary eutectic phases are distributed in α phase boundaries. Also, Mg_2Si precipitates are visible in some regions inside the α grains and at the α grain boundaries. Microstructures of stir casted composites with different amounts of TiB_2 reinforcement are illustrated in Figs. 4(b)–(d). In these micrographs, TiB_2 particles are distinguished as white areas surrounded by α matrix. As it is seen, the contents of reinforcements are increased in microstructure that is in accordance with the increasing amount of particles in molten aluminum during stir casting. As the stir casting parameters were optimized before production of samples, the minimum fraction of porosities and particle agglomerations is observable. Also, the reinforcement / matrix interfaces are approximately free of porosity due to the improvement of wettability by adding K_2TiF_6 and preheating of TiB_2 particles just before adding to the melt. Fig. 5 shows SEM images of as-cast Al-6061 matrix alloy after etching. Fig. 5(a) represents that Mg_2Si precipitates are formed as thin black layers in α grain boundary. Also, the Al-Mg-Si ternary eutectic is mainly located at grain boundary triple junctions. Fig. 5(b) shows the eutectic regions at higher magnification that appear as dendrites during final stages of solidification. Scanning electron micrographs of as-cast composite are also represented in Fig. 6. As can be seen, TiB_2 ceramic particles were also incorporated in microstructure and located at grains interiors and mostly at grain boundaries. Fig. 6(b) illustrates TiB_2 particle at higher magnification. As mentioned before, K_2TiF_6 was mixed with TiB_2 particles for increasing the wettability of reinforcement particle with liquid aluminum. In this condition, K_2TiF_6 reacts with aluminum according to the following expression [27]:

$$3K_2TiF_6 + 13Al \rightarrow 3Al_3Ti + 3KAlF_4 + K_3AlF_6 \quad (1)$$

The main product of this reaction is Al_3Ti compound that appears in the flake form at TiB_2 and matrix interface (Fig. 6(b)). As the mixture of TiB_2 and K_2TiF_6 was preheated at 250 °C for 2 h in electric furnace under oxidizing environment, it is expected that a very thin layer of B_2O_3 and TiO_2 oxides are formed on the surface of TiB_2 particles before adding to the melt. Liquid Al can react with these oxides and fine in situ TiB_2 will be formed according to the following reactions [28,29]:

$$3Al + B_2O_3 \rightarrow Al_2O_3 + AlB_2 \quad (2)$$

$$13Al + 3TiO_2 \rightarrow 2Al_2O_3 + 6Al_3Ti \quad (3)$$

$$AlB_2 + Al_3Ti \rightarrow Al + TiB_2 \quad (4)$$

As it is seen in Fig. 6(b), very fine in situ TiB_2, AlB_2 blocks and Al_3Ti flakes are observable on the surface and around primary TiB_2 particle. Also, as can be seen in Fig. 6(a), TiB_2 particles are distributed in both transgranular and intergranular regions. Furthermore, the images shown in Fig. 6(c) and (d) indicate good bonding between the matrix and ceramic particles. In fact, it seems that probably the reaction between aluminum and TiB_2 reinforcements results in the formation of a strong bond in the Al/TiB_2 interface. Fig. 7 shows the results of energy dispersive spectroscopy (EDS- mapping) analysis. According to these results, it can be clearly seen that there are two different color phases: one is a very dark boride rich region, which is predominantly TiB_2 and the other lighter region is aluminum matrix. Also, the results of elemental mapping confirmed the distribution of Al, Si, Mg, B and Ti in the composite with 9 wt% TiB_2. X-ray diffraction patterns from as stir casted Al-6061 matrix alloy and fabricated composites are shown in Fig. 8. As can be seen, only aluminum, Mg_2Si and Al_5FeSi peaks are observable in diffraction pattern of Al6061 matrix alloy. In the case of Al6061-TiB_2 composites the TiB_2, AlB_2 and Al_3Ti compounds were also detected in addition to Al6061 phases. It is evident that more peaks are appeared and the intensity of TiB_2, AlB_2 and Al_3Ti peaks is increased with the increase of reinforcement fraction. Therefore, the result of X-ray diffraction analysis demonstrates the occurrence of aforementioned reactions and is in accordance with the SEM observations showing different reaction products in the vicinity of TiB_2 particles (Fig. 6(b)).

3.2. Mechanical properties

3.2.1. Micro-hardness

Fig. 9 represents the micro-hardness of matrix Al6061 and Al6061-TiB_2 composites produced by stir casting technique. Results of micro-hardness mea-

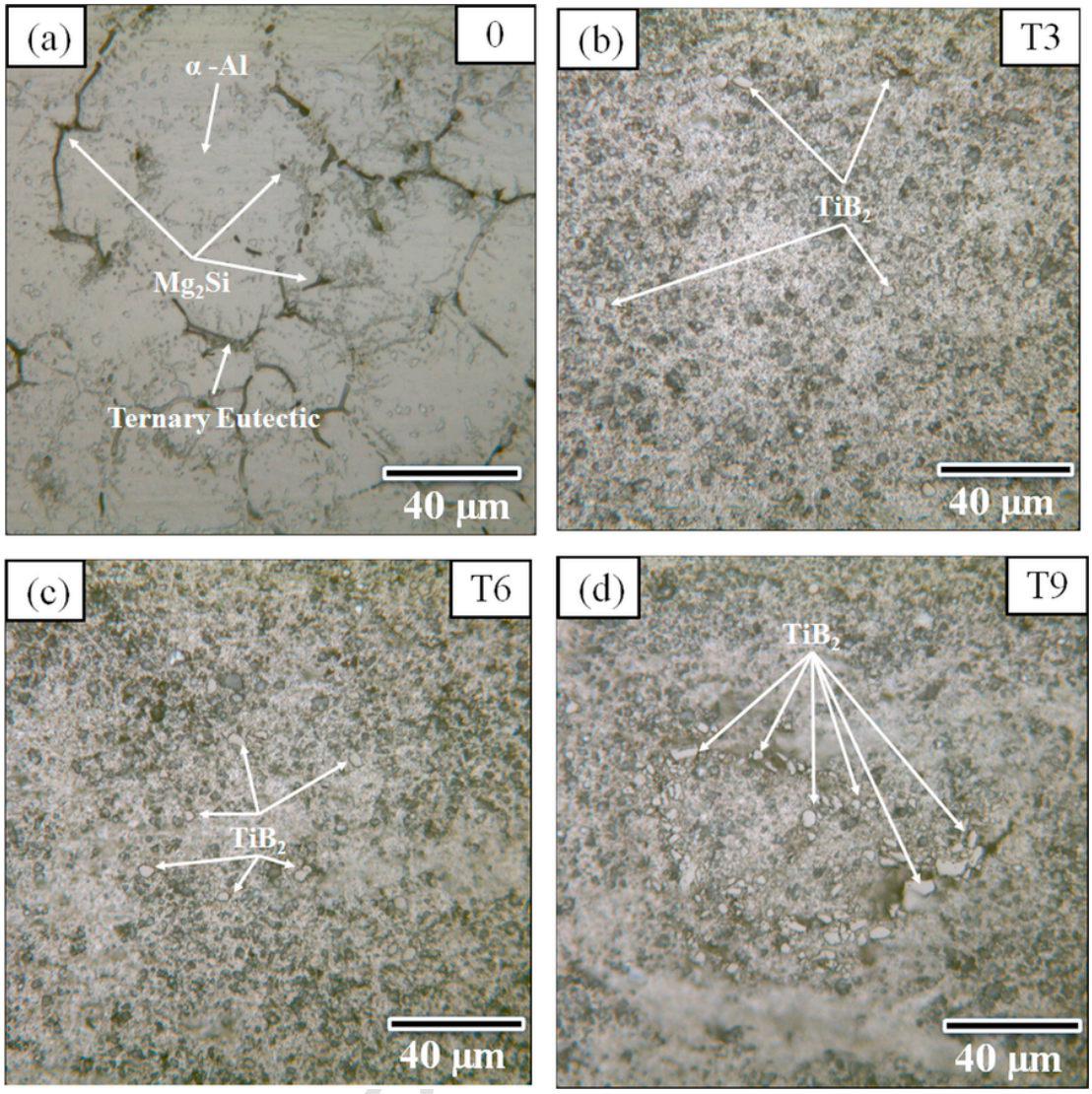

Fig. 4. Optical microstructure of as stir cast: (a) Al6061 Matrix, (b) Al6061-3 wt%. TiB_2, (c) Al6061-6 wt%. TiB_2 and (d) Al6061-9 wt%. TiB_2.

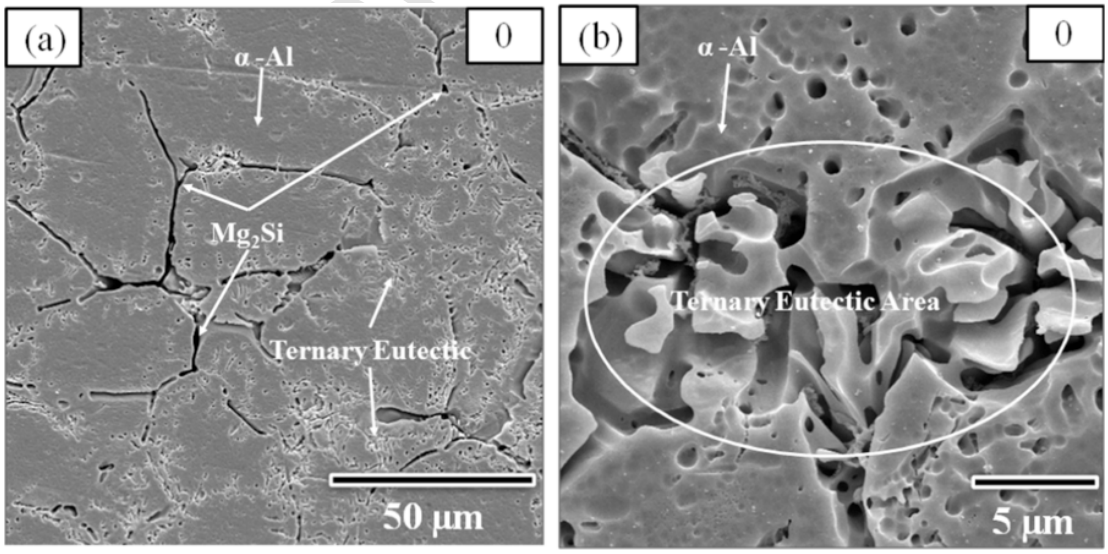

Fig. 5. SEM micrographs of as-cast Al6061 matrix (a) at low magnification and (b) high magnification.

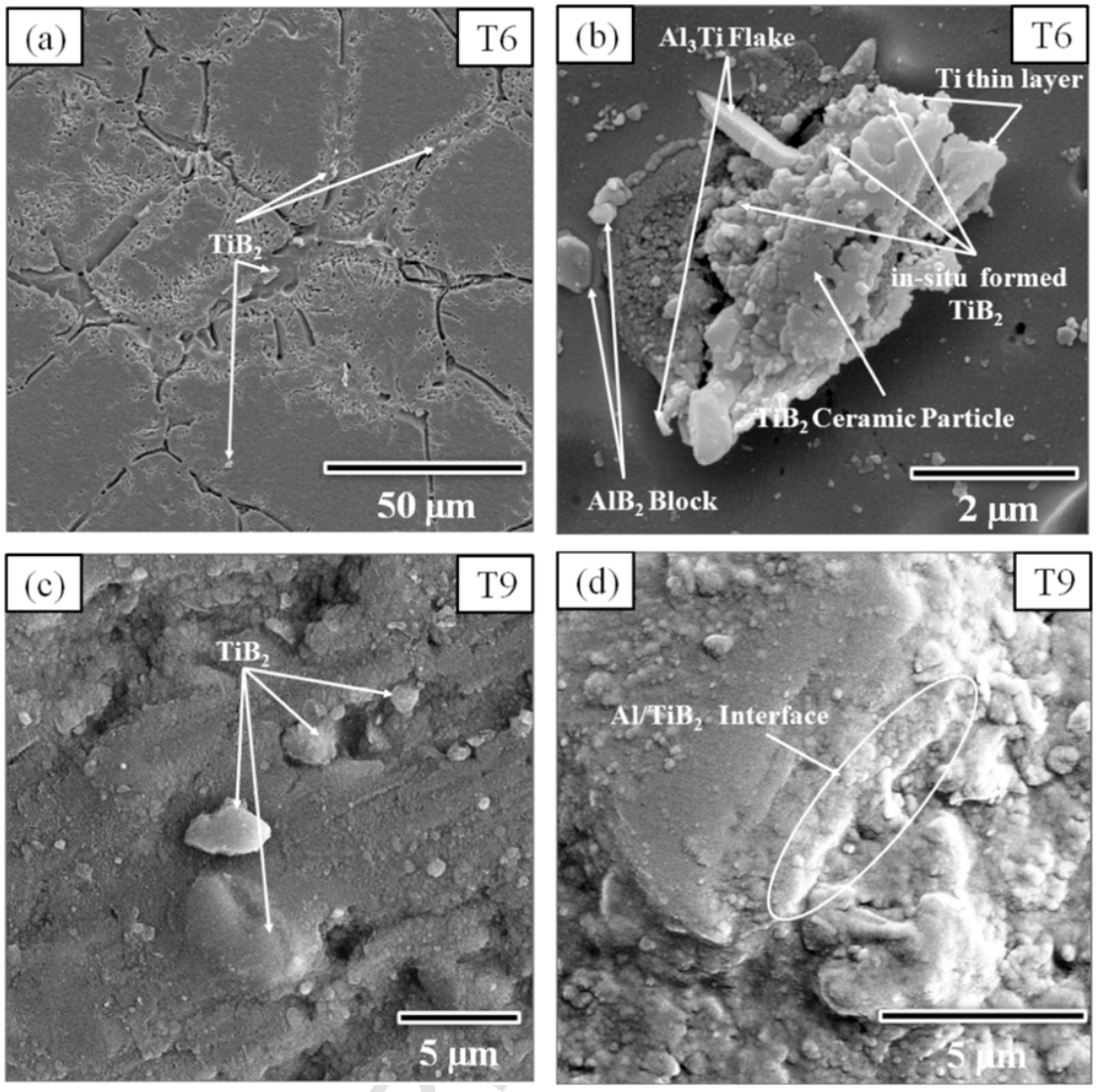

Fig. 6. SEM micrographs of as-cast composites: (a, b) Al6061-6 wt%. TiB_2 and (c, d) Al6061-9 wt%. TiB_2.

surements reveal a pronounced increase in hardness with increasing volume fraction of TiB_2 reinforcement in matrix. With increase of TiB_2 content, the micro-hardness of T3, T6 and T9 samples increased by about 44.7%, 47.3% and 51.3%, respectively, compared to the unreinforced sample. It has been proved that the incorporation of hard reinforcement into ductile matrix increases the hardness by different mechanisms. TiB_2 particles have higher hardness and stiffness compared with Al6061 matrix and enhances its resistance to plastic deformation. Also, the hardness of composite is increased by decreasing grain size of matrix material. Adding TiB_2 particles in to Al6061 melt during stir casting provides preferred sites for heterogeneous nucleation of matrix grains. Therefore, matrix microstructure is refined by increasing the volume fraction of TiB_2 particles. This is one of the reasons for increasing hardness with the increase of reinforcement volume fraction. The other major factor that greatly influences the hardness of composites is the bonding characteristics of reinforcement particles and matrix material. Therefore, the wetting angle between matrix and reinforcement and the atomic nature of the interface affect the load transfer capacity of matrix to reinforcement. It must be noted that TiB_2 is stable in molten aluminum and don't form brittle reaction layers. Finally, the free Ti resulted from decomposition of K_2TiF_6 reacts with aluminum to form hard and brittle Al_3Ti intermetallic phase. Therefore, the formation of Al_3Ti intermetallic is another cause of the improved hardness of Al6061-TiB_2 composites compared with Al6061 matrix alloy.

3.2.2. Tensile/Bending strength and elongation

Tensile engineering stress- engineering strain curves of Al6061 matrix and Al6061-TiB_2 composites are shown in Fig. 10. As it is seen Al6061 has a lower strength and higher elongation than fabricated composites. As it is evident, all curves show a similar trend. After sharp increase in stress levels at the beginning of tensile deformation, the work hardening is decreased continuously and reaches to zero where maximum stress is attained. As all of the investigated samples are in stir casted state, the microstructures have low dislocation densities compared with materials produced by solid-state processing techniques. The work hardening capacity of Al6061 and Al6061-TiB_2 composites are high enough to show considerable plastic strain before necking. Fig. 11 shows the variation of ultimate tensile strength (σ_{UTS}) and elongation percentage of synthesized Al6061-TiB_2 composites as a function of the volume fraction of TiB_2 particles. As it is seen, the ultimate tensile strength of all composites is higher than Al6061 matrix and their magnitudes are increased with the increase of TiB_2 volume fraction without significant degradation of elongation to failure. Also, the ultimate tensile strength of Al6061-9 wt% TiB_2 is 257 MPa, which is 29.2% higher than that for Al6061 alloy. Effect of TiB_2 addition on strength of Al6061-TiB_2 composites can be described through two different approaches. One is based on the transfer of load from matrix to reinforcement particles in which the bonding quality is of great importance and the second is based on the effect of reinforcement particles on yield strength of matrix phase. According

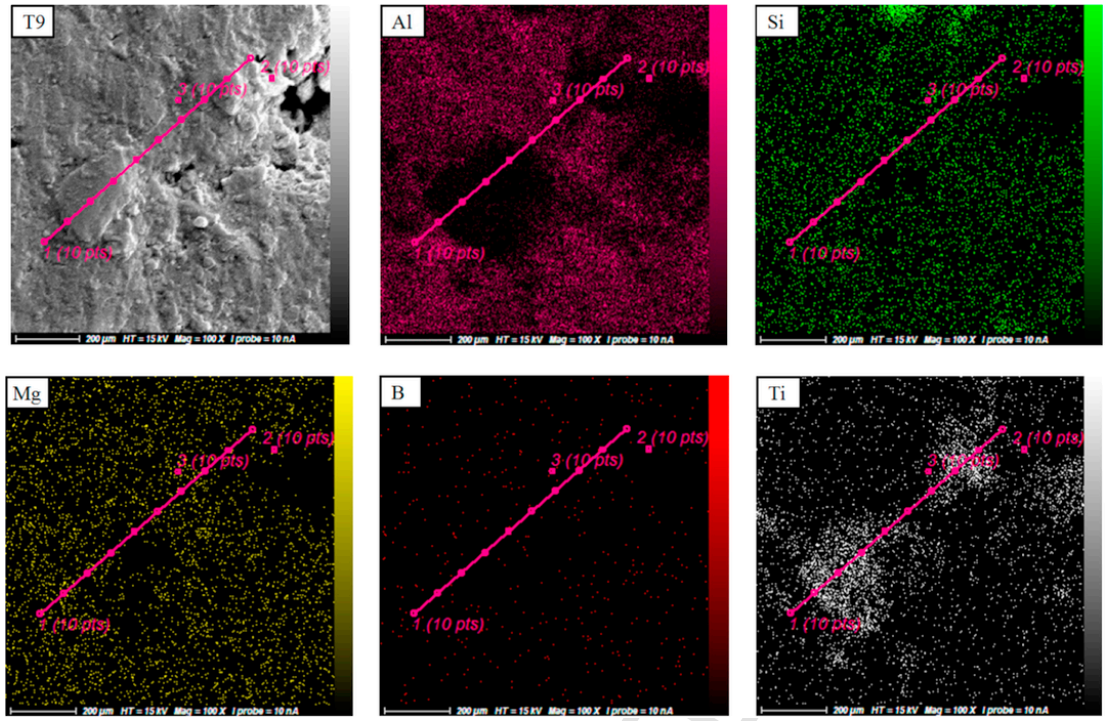

Fig. 7. The EDS- mapping results of Al6061- 9 wt% TiB_2.

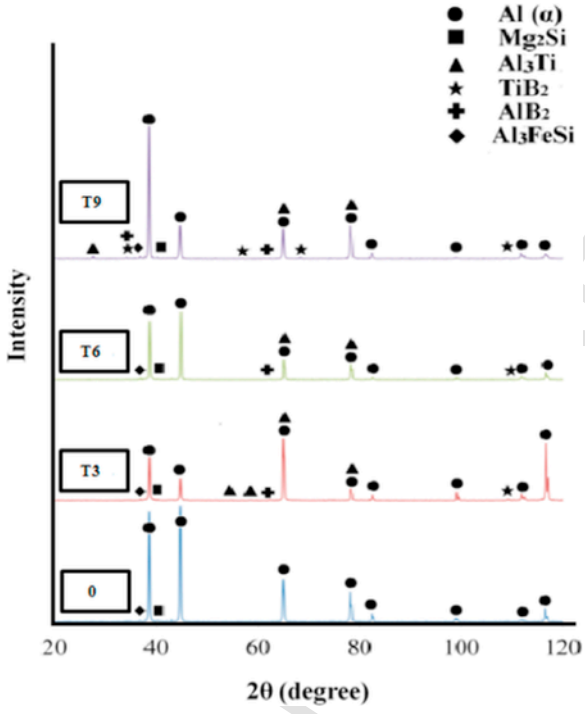

Fig. 8. X-ray diffraction patterns of Al6061 matrix and Al6061-TiB_2 composites.

to the first approach, the yield strength of composite can be described as a function of the volume fraction of reinforcement through the following expression [30]:

$$\sigma_{yc} = \sigma_{ym}\left[V_p(1 + s/2) + (1 - V_p)\right] \quad (5)$$

where V_p is the volume fraction of reinforcement, S is the aspect ratio of particles, σ_{ym} is the yield strength of matrix and σ_{yc} is the yield strength of composite. As it is seen, increasing the amount of reinforcement improves the

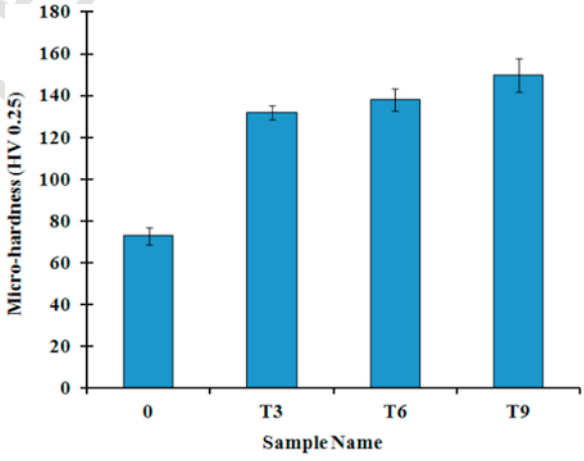

Fig. 9. Micro-hardness of as-cast Al6061 and Al6061-TiB_2 composites.

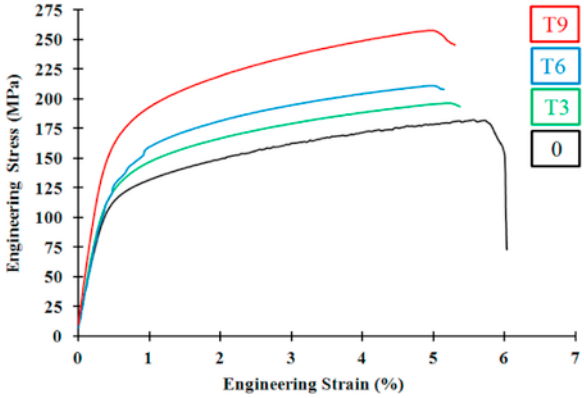

Fig. 10. Engineering stress-strain curves of as-cast Al6061 and Al6061-TiB_2 composites.

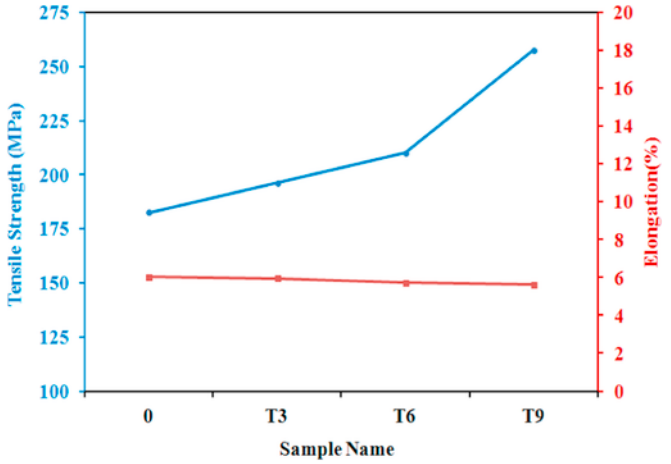

Fig. 11. Variations of tensile strength and elongation percentage of as-cast Al6061 alloy containing different amounts of TiB_2.

load bearing capacity and therefore contributes to composites yield strength increment. Second approach includes three different mechanisms: first mechanism is the grain refinement of matrix by incorporating TiB_2 particles into matrix phase (Hall-Petch effect). It has been fully realized that the grain boundaries act as obstacles for dislocation movement [31] and thereby lead to the increase of yield stress. TiB_2 particles suppress grain growth of matrix phase and enhance the area fraction of grain boundaries. Second mechanism is the Orowan strengthening effect of TiB_2 particles. According to this mechanism, high volume fraction of fine and un-sharable TiB_2 particles, distributed uniformly in the ductile matrix, can act as obstacles for dislocation movement. Therefore, dislocation loops formed around reinforcement particles raise the stress required for more deformation. Third is the dislocation formation due to the difference in thermal expansion coefficients of reinforcement and matrix. Thus, increased dislocation density in matrix by these phenomena makes deformation more difficult which results in higher yield strength. Fig. 12 represents the variation of flexural strength of Al6061-TiB_2 composites with volume fraction of reinforcement particle which were measured using three point bending

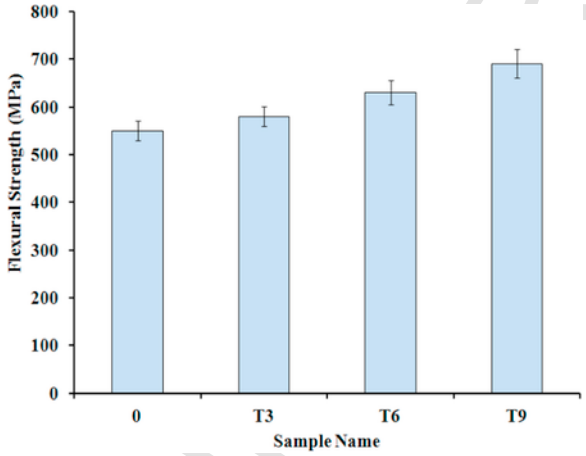

Fig. 12. Variations of flexural strength of as-cast Al6061 alloy containing different amounts of TiB_2.

test. As it is evident the bending strength of composites is increased with the increase of reinforcement fraction and reaches to 690 MPa in the case of Al606-9 wt%. TiB_2.

3.3. Fractography

Fig. 13 represents SEM micrographs from the fracture surfaces of Al6061 alloy and Al6061-TiB_2 composite samples after tensile testing at room temperature. As can be seen, some deep equiaxed dimples existed in fracture surface of Al6061 alloy (Fig. 13(a)) indicating the occurrence of large plastic deformation just before failure. Therefore, the fracture of Al6061 alloy is deduced to be ductile and occurred by the formation and coalescence of micro-voids. It can be said that during tensile testing, the formation of micro-voids are initiated under the local three dimensional state of stress and grow by rising tensile load. Finally, the voids reach to a critical size and fracture is occurred by coalescence of such micro-voids. The fracture surfaces of Al6061-3 wt% TiB_2 composites consist of deep dimples indicating a higher amount of plastic deformation before fracture and the cleavage facets at some area (Fig. 13(b)). It is concluded that cracks are initiated from the interface of matrix and TiB_2 particles and propagate along the boundary. Inspection of the fracture surface of Al6061-9 wt% . TiB_2 composites (Fig. 13(c)) shows shallower dimples compared with Al6061-3 wt%. indicating a lower plastic deformation before fracture. Therefore, fracture surfaces of Al6061-TiB_2 composites show a ductile feature of Al6061 matrix. Also, there are some cleavage features indicating the crack development at the interface of Aluminum matrix and TiB_2 particles due to stress concentration at these regions. Fig. 13(d) demonstrates the fracture surface of Al6061-9 wt%. TiB_2 composites at higher magnification. Some TiB_2 ceramic particles are visible that is the evidence of the growth of cracks from reinforcement and matrix interface. It is concluded that the ductility of composites is decreased by increasing the fraction of TiB_2 reinforcement particulates.

4. Conclusions

In the present study Al6061 composite reinforced with different amounts of TiB_2 reinforcement particles were synthesized by stir casting method. Microstructure and mechanical properties of fabricated composites were analyzed and the following conclusions were made:

1. A uniform distribution of reinforcements in aluminum matrix without agglomeration were achieved by optimizing process parameters and strong bonding were observed to be attained by K_2TiF_6 addition and preheating of reinforcing TiB_2 powders before adding to the melt.
2. Tensile strength of fabricated composites was improved by increasing the volume fraction of TiB_2 reinforcement particles without significant decrease of elongation to failure.
3. Improved mechanical properties of Al6061-TiB_2 composites compared with matrix Al6061 alloy is due to the high load bearing capacity of reinforcement particle, decreasing matrix grain size, interaction of dislocations with reinforcement particles by Orowan mechanism and generated dislocations as a result of difference between thermal expansion coefficients of matrix and reinforcements.
4. Fracture surfaces of Al6061 matrix alloy and Al-TiB_2 composites are consisted of dimples which indicate that ductile rupture is the predominant fracture mechanism. The depth of dimples was decreased with increasing volume fraction of reinforcement particles and some cleavage facets were observed in the fracture surface of Al6061-TiB_2 composites.

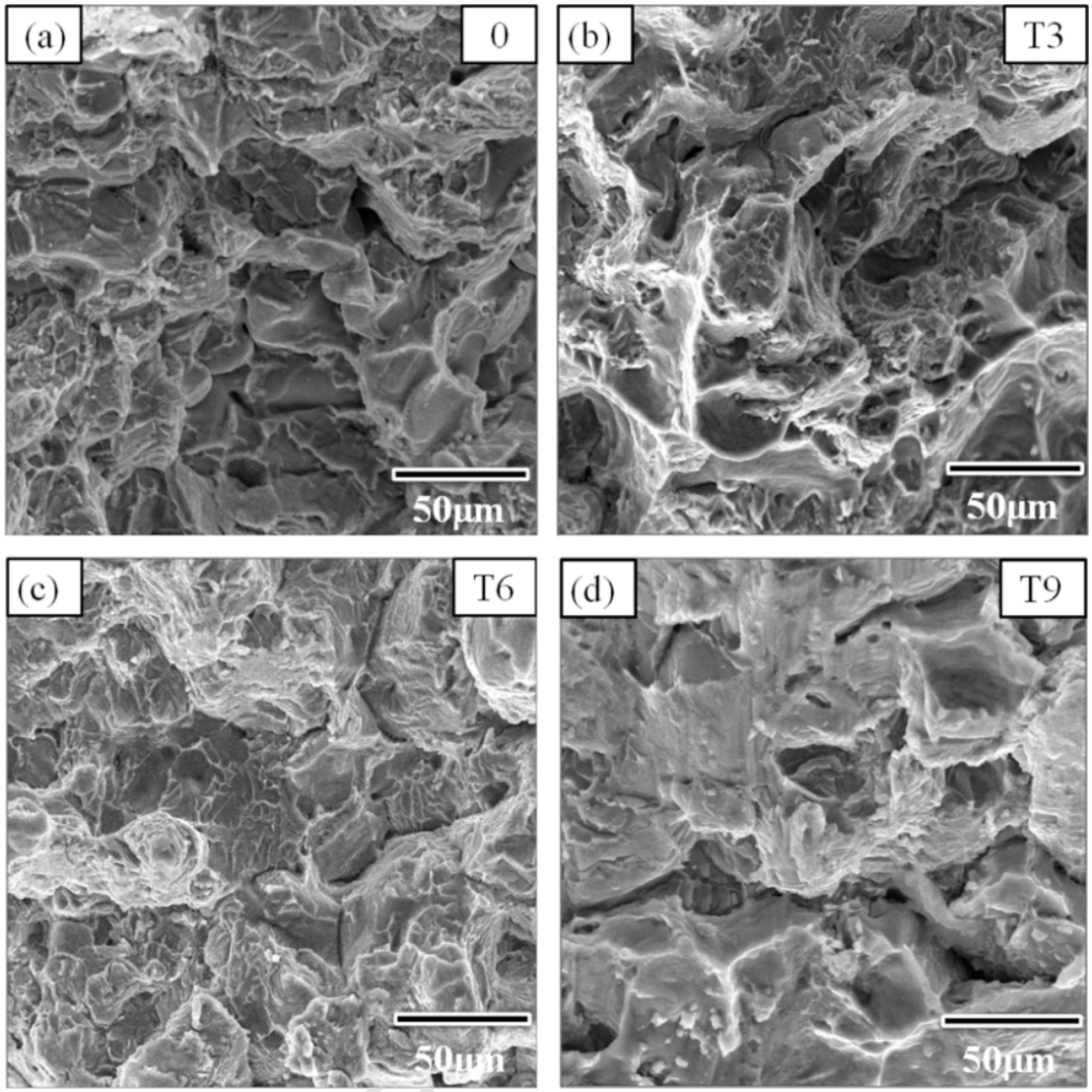

Fig. 13. SEM micrographs taken from the fracture surfaces of tensile specimens: (a) Al 6061 matrix, (b) Al6061-3 wt%. TiB_2, (c) Al6061-6 wt%. TiB_2 and (d) Al6061-9 wt%. TiB_2.

References

[1] D.B. Miracle, Metal matrix composites- from science to technological significance, Compos. Sci. Technol. 65 (2005) 2526–2540.

[2] J.W. Kaczmar, K. Pietrzak, W. Wlosinski, The production and application of metal matrix composite materials, J. Mater. Process. Technol. 106 (2000) 58–67.

[3] S. Rawal, Metal-matrix composites for space applications, JOM (2001) 14–17.

[4] I.G. Waston, M.F. Forster, P.D. Lee, R.J. Dashwood, R.W. Hamilton, A. Chirazi, Investigation of the clustering behavior of titanium diboride particles in aluminum, Composite: Part A 36 (2005) 1177–1187.

[5] P. Baldus, M. Janson, D. Sporn, Ceramic fiber for matrix composites in high temperature engine applications, Science 285 (1999) 699–703.

[6] F. Akhtar, Microstructure evolution and wear properties of in situ synthesized TiB_2 and TiC reinforced steel matrix composites, J. Alloy. Compd. 459 (2008) 491–497.

[7] S.F. Moustafa, Z. Abdel-Hamid, A.M. Abd-Elhay, Copper matrix SiC and Al_2O_3 particulate composites by powder metallurgy technique, Mater. Lett. 53 (2002) 244–249.

[8] Q.C. Jiang, H.Y. Wang, B.X. Ma, Y. Wang, F. Zhao, Fabrication of B_4C particulate reinforced magnesium matrix composite by powder metallurgy, J. Alloy. Compd. 386 (2005) 177–181.

[9] S. Gopalakrishnan, N. Murugari, Production and wear characterization of AA 6061 matrix titanium diboride particulate reinforced composite by enhanced stir casting method, Composite: Part B 43 (2012) 302–308.

[10] R.D. Haghighi, S.A. Jahromi, A. Moresedgh, M.T. Khorshid, A compersion between ECAP and conventional extrusion for consolidation of aluminum metal matrix composite, J. Mater. Eng. Perform. 21 (2012) 1885–1892.

[11] R.S. Mishra, Z.Y. Ma, I. Charit, Friction stir processing: a novel technique for fabrication of surface composite, Mater. Sci. Eng. A 341 (2003) 307–310.

[12] J.M. Torralba, C.E. Costa, F. Velasco, P/M aluminum matrix composites: an overview, J. Mater. Process. Technol. 133 (2003) 203–206.

[13] H. Aydin, A. Bayram, A. Uguz, K.S. Akay, Tensile properties of friction stir welded joints of 2024 aluminum alloy in different heat treated state, Mater. Des. 30 (2009) 2211–2221.

[14] Y.C. Kang, S.L. Chan, Tensile properties of nanometric Al_2O_3 particulate reinforced aluminum matrix composites, Mater. Chem. Phys. 85 (2004) 438–443.

[15] A. Sabahi Namini, M. Azadbeh, M. Shahedi Asl, Effect of TiB_2 content on the characteristics of spark plasma sintered Ti–TiB_w composites, Adv. Powder Technol. 28 (2017) 1564–1572.

[16] R. Tyagi, Synthesis and tribological characterization of in situ cast Al-TiC composites, Wear 259 (2005) 569–576.

[17] K.B. Lee, H.S. Sim, H. Kwon, H. Kwon, S.Y. Cho, Tensile properties of 5052 al matrix composites reinforced with B_4C particles, Metall. Mater. Trans. A 32 (2001) 2142–2147.

[18] Z.Y. Chen, Y.Y. Chen, G.Y. An, Q. Shu, D. Li, Y.Y. Liu, Microstructure and properties of in situ Al/TiB_2 composite fabricated by in-melt reaction method, Metall. Mater. Trans. A 31 (2000) 1959–1964.

[19] M. Rahimian, N. Ehsani, N. Parvin, H.R. Baharvandi, The effect of particle size, sintering temperature and sintering time on the properties of Al-Al_2O_3 composites, made by powder metallurgy, J. Mater. Process. Technol. 209 (2009) 5387–5393.

[20] M. Alizadeh, M.H. Paydar, Fabrication of nanostructure Al/SiC composite by accumulative roll bonding, J. Alloy. Compd. 492 (2010) 231–235.

[21] L.M. Tham, M. Gupta, L. Cheng, Predicting the failure strains of Al/SiC composites with reacted matrix-reinforcement interfaces, Mater. Sci. Eng. A 354 (2003) 369–376.

[22] J.M. Gomez Salazar, A. Soria, M.I. Barrena, Wlding of AA6061-(Al_2O_3) composite: effect of weld process variables and post welding heat treatment on microstructure and mechanical properties, Sci. Technol. Weld. Join. 10 (2005) 339–343.

[23] M. Karbalaei Akbari, H.R. Baharvandi, K. Shirvanimoghaddam, Tensile and fracture behavior of nano/micro TiB_2 particle reinforced casting A356 aluminum alloy composites, Mater. Des. 66A (2015) 150–161.

[24] K. Shirvanimoghaddam, H. Khayyam, H. Abdizadeh, M. Karbalaei Akbari, A.H. Pakseresht, E. Ghasali, M. Naebe, Boron carbide reinforced aluminium matrix composite: physical, mechanical characterization and mathematical modeling, Mater. Sci. Eng.: A 658 (2016) 135–149.

[25] V. Auradi, G.L. Rajesh, S.A. Kori, Processing of B_4C Particulate Reinforced 6061Aluminum Matrix Composites by melt stirring involving two-step addition, Procedia Mater. Sci. 6 (2014) 1068–1076.
[26] P. Mogilevsky, E.Y. Gutmanas, I. Gotman, R. Telle, Reactive formation of coatings at boron carbide interface with Ti and Cr powders, J. Eur. Ceram. Soc. 15 (6) (1995) 527–535.
[27] F. Chen, Z. Chen, F. Mao, T. Wang, Z. Cao, TiB_2 reinforced aluminum based in situ composites fabricated by stir casting, Mater. Sci. Eng.: A 625 (2015) 357–368.
[28] H.G. Zhu, H.Z. Wang, L.Q. Ge, S. Chen, S.Q. Wu, Formation of composites fabricated by exothermic dispersion reaction in Al-TiO_2-B_2O_3 system, Trans. Nonferrous Met. Soc. China 17 (2007) 590–594.
[29] H. Hosoda, T. Inamura, T. Shimoyamada, H. Noma, K. Wakashima, Phase reactions of Al-Ti-B ternary and Al-Ti-B-O quaternary systems for Al-based metal matrix composites, in: Proceedings of the 12th International Conference on Aluminium Alloys, September 5–9, 2010, pp. 2051–2056.
[30] S. Jayalakshmi, S. Gupta, S. Sankaranarayana, S. Sahu, M. Gupta, Structural and mechanical properties of Ni60Nb40 amorphous alloy particle reinforced Al-based composites produced by microwave-assisted rapid sintering, Mater. Sci. Eng.: A 581 (2013) 119–127.
[31] N. Hansen, Hall-Petch relation and boundary strengthening, Scr. Mater. 51 (2004) 801–806.